❏   21

Electrostatic precipitator design with wire-cylinder electrodes as a particulate matter reduction

Yulianta Siregar, Bio Debataraja, Soeharwinto, Naemah Mubarakah, Riswan Dinzi
Department of Electrical Engineering, Universitas Sumatera Utara, North Sumatera, Indonesia

Article Info

ABSTRACT

Small industries are inseparable from the production of gaseous pollutants. One of the contents of exhaust gases produced from small industrial activities is particulate matter. The consequences of exposure to particulate matter for too long are coughing, cancer, blood coagulation, and death. For this reason, a tool is needed to capture particulate matter in small industrial exhaust gases. Based on the problems described, this research proposes using the electrostatic precipitator with the cockroft-walton method because this method is very effective in capturing particulate matter. The research results on electrostatic precipitator (ESP) with a pair of electrodes will achieve an efficiency of 25.4% when the voltage regulator is 20 V, while the efficiency is 98.7% when the voltage regulator is 35 V. The ESP with two pairs of electrodes will achieve 99.5% efficiency when the voltage regulator is 30 volts. Installing a vibrator as a particle thresher at the electrode is unsuitable for low-temperature exhaust gases because it produces a liquid and sticky residue that makes it difficult to fall off.
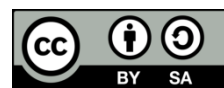
Corresponding Author:

Yulianta Siregar
Department of Electrical Engineering, Faculty of Engineering, Universitas Sumatera Utara
20222 Medan, North Sumatera, Indonesia
Email: julianta_srg@usu.ac.id

1. INTRODUCTION

Small industries are inseparable from the production of pollutants, both solid, liquid, and gaseous pollutants. Air pollution is an atmospheric condition where the presence of substances with concentrations exceeding normal ambient limits can have an impact on humans, animals, and vegetation. Examples of hazardous compounds found in industrial exhaust gases are sulfur (SOx) [1], [2], nitrogen components (NOx) [3]–[5], carbon (Cox) [6], [7], and particulate matter (PM) [4], [8]. Particulate matter (PM) is a very dangerous solid emission particle where the level of danger from PM depends on its diameter. The smaller the size of the PM, the more dangerous it is because it is easier to enter the lungs' respiratory tract. Examples of dangerous diseases caused by PM are bronchitis, acute respiratory infection, cancer, asthma, decreased lung function, and premature death. From the problems discussed, a tool is needed to overcome the exhaust gas problem, especially particulate matter, to prevent air pollution. A tool is needed to capture the exhaust gas particles to prevent air pollution due to waste burning and small industrial production processes. It is hoped that the tools that will be made later are easy and inexpensive to operate, efficient in size, have relatively inexpensive manufacturing costs, and have high particle capture efficiency. Small industries such as hospitals, rice mills, and welding workshops can reduce air pollution with this tool.

A very effective method for capturing particulate matter in flue gas is the electrostatic precipitator (ESP) method. The electrostatic precipitator method works by flowing the smoke from combustion into an electric field area rich in free charge between the discharge electrode (DE) and the collector electrode (CE).

The discharge electrode functions as ionizing the particles contained in the combustion exhaust gas so that the exhaust gas particles have a charge. The collector electrode is an attractant for charged particles that have been ionized by the discharge electrode so that these particles gather and settle on the collector electrode plate [9], [10]. With this process, the harmful particles in the smoke produced by combustion can be eliminated or reduced. ESP experiments have been carried out, such as designing an electrostatic precipitator as a subsystem in capturing spray pyrolysis particles [11], [12] and designing an air purifier using a voltage multiplier application [13]–[15]. Both experiments used a flyback transformer with positive polarity as a high-voltage power generator. High voltage with positive polarity will produce a positive corona, while high voltage with negative polarity will produce a negative corona. There is a significant difference between positive and negative coronas, namely the distribution of the density of the number of electrons and the effect of temperature. The total number of electrons in a negative corona is 50 times that of a positive corona. The electron density in the negative corona area is four times greater than that of the positive corona. A positive corona decreases the number of electrons when there is an increase in temperature. Whereas in a negative corona, the number of electrons will increase if there is an increase in temperature [16], [17]. Another difference between positive and negative coronas is the breakdown voltage. The breakdown voltage indicates that the electric field is no longer homogeneous, which causes a decrease in the efficiency of the ESP. In the positive corona, the breakdown voltage will occur before the negative corona. Negative corona has more advantages than positive corona when applied to ESP because the number of free ions produced is greater. So, this study used a negative corona as a generator of electron ions. Negative coronas require high voltage with negative polarity. In the experiment, a high voltage with negative polarity will be generated by the walton-cockroft circuit [18]. Further, the next difference is that the electrodes used are of the wire-cylinder type. This was chosen because using wire cylinder electrodes makes it easier to maintain, and the design is simpler than other types of electrodes to reduce construction costs. The cylinder electrode can function as a filter and a chimney.

An electrostatic precipitator is a tool that functions to filter exhaust gases, especially particulate matter. Particulate matter levels in industrial exhaust gases have been regulated in the regulation of the minister of environment and Forestry of the Republic of Indonesia [19], [20]. It concerns emission quality standards for businesses and/or cement industry activities which states that the industry cement has the potential to cause air pollution. So, it is necessary to control exhaust emissions. This regulation can be used as a reference in determining the performance of ESP. The permitted particulate content from industrial activities is 150 (mg/Nm)^3 or, if converted to 120 ppm. Because of this, the ESP that will be made later must be able to follow the quality standard levels that the government has made. At any time, the levels of particulate matter must be monitored to prevent air pollution. If the ESP is continuously exposed to particles for a long time, the performance of the ESP will decrease. A tool is needed that can clean the electrodes from adhering particles when the ESP is operating to maintain the ESP's performance. An electrode vibrator is a tool that generates vibrations on the collector electrode with the aim of knocking out the attached particles so that the particles fall due to gravity. So, this study designed an electrode vibrator on the ESP.

2. METHOD
2.1. Smoke-producing room design
In this study, ESP testing used smoke produced from burning egg trays. The egg tray is burned, then the fire is turned off and only small embers remain on the egg tray. An egg tray that has small smoldering coals will produce smoke. This smoke was used as a test on ESP. The egg tray containing the coals was placed in a room of acrylic 40×40×30 cm. The smoke generated in the room will be channeled to the ESP using a fan. The smoke generated by burning egg trays is considered a minor industrial exhaust gas.

2.2. Design of electrostatic precipitator
The ESP type used in this experiment is the one-stage type where the discharge electrode and collector electrode are located in the same area. Furthermore, the loading and particle capture processes are in the same electric fields. The collector electrode is made of stainless steel and is used in the form of a cylinder with a diameter of 6 cm. While the discharge electrode used has a diameter of 0.04 cm and is made of copper wire. In determining the ESP dimensions, it is first necessary to determine and define some of the parameters used. The parameters used in the design can be seen in Table 1 [21]–[24].

By setting the parameters used, other variables are obtained as follows [10], [25], [26]:
- Relative density of air.

$$\delta = \frac{298}{273+T} \times \frac{P}{760}$$
$$\delta = \frac{298}{273} \cdot \frac{760}{760} = 0.968$$

(1)

- Corona discharge electric field.

$$E_c = 31.\delta \left[1 + \frac{0.308}{\sqrt{\delta.r_1}}\right]$$

$$E_C = 31 \times (0.968) \left(1 + \frac{0.308}{\sqrt{(0.968)\times(0.02)}}\right) = 96.403 \; kV/cm$$

(2)

- Corona discharge voltage.

$$V_C = E_C \times r_1 \times ln\left(\frac{r_2}{r_1}\right)$$

$$V_C = (96.403) \times (0.02) \times ln\left(\frac{3}{0.02}\right) = 9.661 \; kV$$

(3)

Table 1. ESP parameters

Parameter	Symbol	Value
Air flow rate	V	0.5 m/s
DE radius	r_1	0.02×10^{-2} m
CE radius	r_2	3×10^{-2} m
Particle diameter	Dp	2.5×10^{-6} m
ESP efficiency	Ƞ	99 %
Temperature	T	308 ^{0}K
Pressure	P	760 mmHg
Dielectric permittivity	ε_0	8.85×10^{-12} F/m
Thermal ion mobility speed	Z_i	1.54×10^{-4} m/Vs
Boltzmann constant	k_B	1.38×10^{-23} J/K
Electron charge	E	1.6×10^{-19} C
Gas Viscosity	μ	1.895×10^{-5} Kg/m. s
Cunningham slip factor	C_c	1.084
Number of pairs of electrodes	N	1 & 2

In these equations, the following variables were used: δ Relative air density, P air pressure (mmHg), E_c electric field strength (kV/cm), T Temperature (^{0}K), V_C Corona initial voltage. Meanwhile, after obtaining the corona discharge voltage, the maximum working voltage is determined. The maximum voltage of the generated corona discharge is 18 kV. The maximum corona discharge current can be obtained for one pair of precipitating electrodes by setting the maximum working voltage.
- Maximum corona discharge current for one pair of electrodes.

$$I = \frac{8\times\pi\times L\times\varepsilon_0\times Z_i}{r_2{}^2\times ln\left(\frac{r_2}{r_1}\right)}V(V - V_c)$$

$$I_c = \frac{8\times(3.14)\times L\times\left(8.85\times10^{-12}\right)\times1.54\times10^{-4}}{3\times10^{-2}\times ln\left(\frac{3\times10^{-2}}{0.02\times10^{-2}}\right)}18000 \times (18000 - 9660.805766)$$

$$I_c = 0.00113958 \; A \times L$$

(4)

- Pseudohomogeneous electric field.

$$E_{ps} = \frac{18000}{3\times10^{-2}} = 600000 \; V$$

(5)

- Ion concentration.

$$N_i = \frac{(0.00113958) \times L}{2 \times (3.14) \times (3 \times 10^{-4}) \times L \times (1.6 \times 10^{-19}) \times (1.54 \times 10^{-4}) \times (600000)}$$

$$N_i = 4.0914 \times 10^{14} \; C$$

- The total amount of charge on the particles per second.

$$n_p = \left(1 + 2\frac{\varepsilon-1}{\varepsilon+2}\right)\left(\frac{E_{ps}.d_p{}^2}{4K_E.e}\right)\left(\frac{\pi.K_E.e.Z_i.N_i}{1+\pi.K_E.e.Z_i.N_i.t}\right) + \frac{d_p.k_B.T}{2.K_E.e^2}\ln\left(1 + \frac{\pi\times K_E\times d_p\times\bar{c_1}\times e^2\times N_i\times t}{2\times k_B\times T}\right)$$

$$n_p = \left\{ \frac{\left(1 + 2\frac{3-1}{3+2}\right)\left(\frac{600000 \cdot (2.5 \times 10^{-6})^2}{4(9 \times 10^9) \cdot (1,6 \times 10^{-19})}\right)}{\left(\frac{\pi \times (9 \times 10^9) \times (1,6 \times 10^{-19}) \times (1.54 \times 10^{-4}) \times (6.054 \times 10^{14}) \times 1}{1 + \pi \cdot (9 \times 10^9) \times (1,6 \times 10^{-19}) \times (1.54 \times 10^{-4}) \times (6.054 \times 10^{14}) \times 1}\right)} \right\} +$$

$$\left\{ \frac{\frac{(2.5 \times 10^{-6}) \times (1,38 \times 10^{-23}) \times 308}{2 \times (9 \times 10^9) \times (1,6 \times 10^{-19})^2}}{ln\left(1 + \frac{\pi \times (9 \times 10^9) \times (2.5 \times 10^{-6}) \times 240 \times (1.6 \times 10^{-19})^2 \times 6.054 \times 10^{14} \cdot 1}{2 \times (1.38 \times 10^{-23}) \times 308}\right)} \right\} \tag{6}$$

$$n_p = 1440.217671$$

- The electric field at CE due to the.

$$U_m = \frac{n_p \times e \times E_{ce} \times C_c}{3\pi \times \mu \times d_p} \tag{7}$$

$$U_m = \frac{1440.217671 \times (1.6 \times 10^{-19}) \times (146355.3602) \times (1.084)}{3\pi(1,895 \times 10^{-5}) \times (2.5 \times 10^{-6})}$$

$$U_m = 0.067024832 \ m/s$$

- The Dautch number is obtained.

$$\eta_f = 100(1 - e^{-De}) \tag{8}$$

$$De = -ln\left(1 - \frac{\eta_f}{100}\right) = -ln\left(1 - \frac{99}{100}\right) = 4.6$$

- The lengths of CE and DE.

$$De = U_m \times \frac{A_c}{Q_g} \tag{9}$$

$$De = U_m \times \frac{2\pi \times r_2 \times L}{v \times \pi \times r_2{}^2}$$

$$L = \frac{De \times v \times r_2}{2 \times U_m} = \frac{(4.6) \times (0.5) \times (3 \times 10^{-2})}{2 \times (0.067024832)} = 0.514734602 \ m \ \approx 0.51m$$

- The corona discharge current of a pair of electrodes.

$$I_c = 0.00113958 \times L = (0.00113958) \times (0.51) = 0.000586581 \ A$$

In these equations, the following variables were used: I effective current (A), V effective voltage (kV), E_{ps} electric field strength at the ESP (V), N_i Ion concentration (C), ε particle dielectric constant (for black carbon particles is 3.0), Z_i Ion electric mobility (1.54x10⁻⁴) m/V$_S$ at 100 °C), K_E electrical constant (9x10⁹), k_B Konstanta Boltzmann (1.38x10⁻²³ J/K), $\overline{C}_l$ average ionic thermal velocity (240 m/s), n_p the amount of charge on the particle, e electron charge (1.60217663x10⁻¹⁹ C), E_{ce} electric field strength near the collecting electrode (V), C_c Cunningham slip factor, μ gas viscosity (Kg/m.s), d_p Particle diameter (m), U_m particle migration rate (m/s), η_f Fractional collection efficiency (%), De deutsch number, A_c collector surface area (m²), Q_g gas flow rate (slpm).

After the calculations have been carried out, the length of a pair of electrodes is 51 cm with a corona discharge current of 0.587 mA and a corona discharge voltage of 18 kV. This study will be analyzed when ESP with a pair of electrodes and two pairs of electrodes. After obtaining the length of the electrode, the maximum corona discharges current, and the number of electrodes, calculations can be carried out to determine the size of the capacitor and the number of levels in the cockroft walton (CW) high voltage generation circuit.

2.3. Design of a high voltage power supply

The voltage source used is 220 volts with a frequency of 50 Hz. The high-voltage power supply circuit consists of 2 voltage generators, namely by using a step-up transformer and a CW voltage multiplier circuit. The ac voltage regulator will control the output voltage. The resulting output voltage must be greater than the initial voltage of the corona discharge, which is 9.7 kV. The magnitude of the working voltage on the electrodes is 51 cm long to obtain a maximum ESP efficiency of 18,000 kV. In testing, the voltage is increased to 28,000 V to overcome the voltage drop caused by the load and increase the variation of the voltage test. In the generation process, the 220 V voltage is increased to 2,000 V with a step-up transformer. Then the output voltage generated by the transformer is multiplied by the walton cockroft circuit [27]. The determining the number of levels.

$$N = \frac{V_0}{2.V_{in}} = \frac{28000}{2.2000} = 7 \qquad (10)$$

The size of the capacitor affects the resulting output voltage because it functions as a storage and discharges the charge to be rectified by the diode. If the output of the CW handle is attached to a load, a voltage drop will occur. In determining the electrode length, the amount of current flowing in the wire-cylinder ESP is 0.000586581 A. Further, the capacitor is a 470 nF mylar capacitor with a storage voltage of up to 2,000 volts.

$$N_{opt} = \sqrt{\frac{V_{max}.f.C}{I}} \qquad (11)$$

$$C = \frac{N_{opt}^2.I}{V_{max}.f} = \frac{7^2.0.000586581}{2000.50} = 287.4 \, nF$$

$$V_{0(max)} = 2.n.V_{max} - \frac{I}{f.c}\frac{2.n^3}{3} \qquad (12)$$

$$V_{0(max)} = 2.7.2000 - \frac{0.000586581}{50.470 \times 10^{-9}}\frac{2.7^3}{3} \cong 22292.3 \, V$$

The maximum output voltage generated when connected to the ESP is 22292.3 V. This voltage has exceeded the desired voltage requirement of 18 kV, which means a 470 nf capacitor can be used as a voltage generator circuit. To produce high voltage with negative polarity can be generated by adjusting the direction of the diode. The high-voltage generator circuit with negative polarity can be made, as shown in Figure 1 [24], [27]. In addition to the influence of the selection of capacitors on voltage generation, other things greatly affect voltage generation, namely the selection of diodes. The selection of a large diode reverses peak voltage smaller than the working voltage will cause damage to the diode. Because the output voltage of the step-up transformer is 2,000 V, a diode with a peak reverse voltage of 2,000 V is needed. The maximum current required by the ESP is 0.587 mA, so a diode is needed that can pass forward currents greater than 0.587 mA. From these specifications, diode CL01 is used with a peak reverse voltage of 12 kV and a forward current of 350 mA. After calculating the dimensions of the combustion chamber, ESP dimensions, and high-voltage power supply, the smoke-producing room and ESP design are carried out. The design of the ESP with a pair of electrodes is depicted in Figure 2. Meanwhile, Figure 2(a) ESP with a pair of electrodes, while Figure 2(b) ESP with two pairs of electrodes. This study was made to see the effect of the number of pairs of electrodes on exhaust gas. The input is the place for artificial gas, the vibrator functions to drop the particles attached to the electrode cylinder, while the output results from the process to produce clean air.
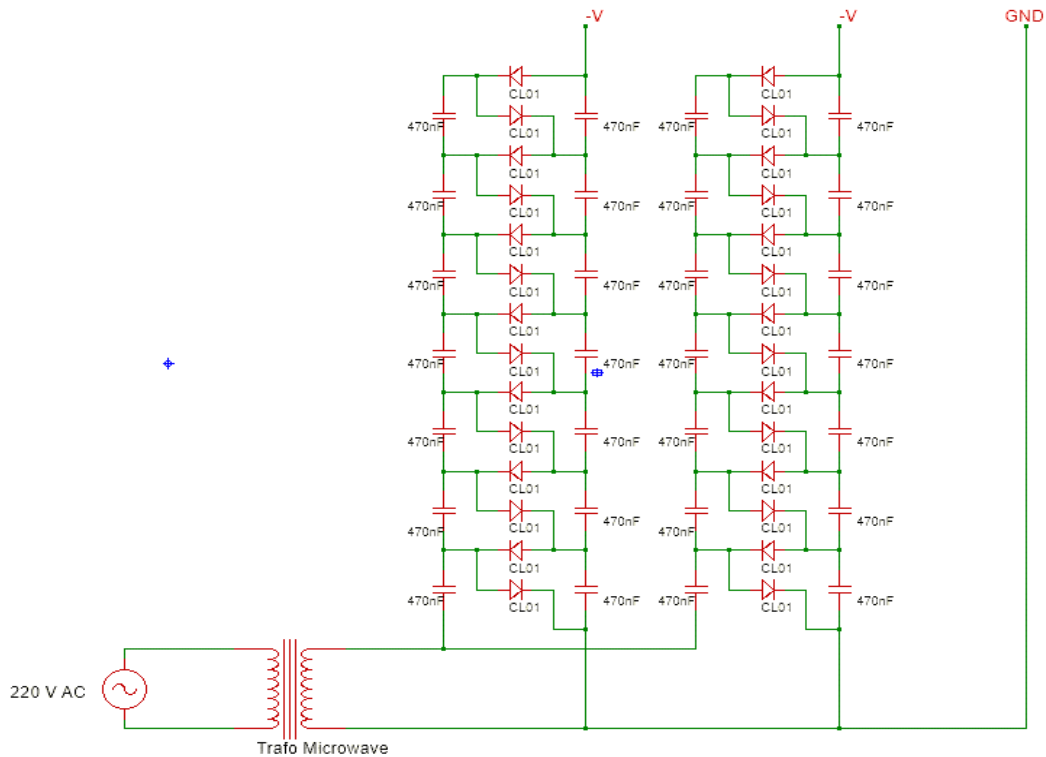

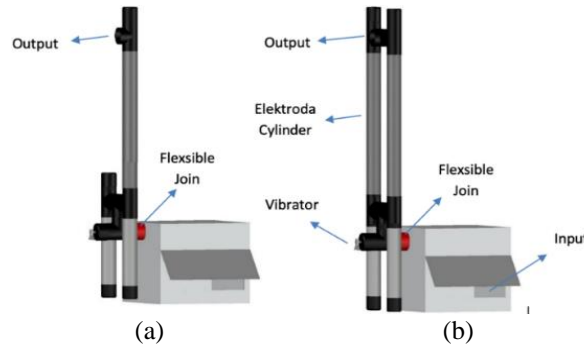Figure 1. The circuit of the high voltage power supply

(a)   (b)

Figure 2. The design of the ESP with a pair of electrodes (a) and (b) two pairs of electrodes

3.   RESULTS AND DISCUSSION

3.1. Testing of negative direct current high voltage

In measuring high voltages, you can use a high-voltage probe. The probe used in this study is the high voltage (HV) 9012 PROBE which has a measurement ratio of 1:1,000, which means that for every 1,000-volt increase, the multimeter will read 1 Volt. Measurements were made by changing the voltage regulator and measuring the voltage generated by the transformer and the output voltage of the CW. The measurement results are presented in Table 2. It explains that by using a 5-volt voltage regulator, we get the transformer voltage, CW voltage without load, and CW voltage connected to the ESP 142 volts, -2.5 kV and -2.1 kV, respectively. Meanwhile, using a 40-volt voltage regulator, we get the transformer voltage, CW voltage without load, and CW voltage connected to the ESP 1156 volts, -22.3 kV and -20.5 kV, respectively. The CW calculation voltage without load is obtained from (3), where the maximum voltage is $V_{\text{transformer}} \times \sqrt{2}$.

Based on the measurement results, the relationship between the increase in the regulator voltage and the change in CW voltage without load, the CW voltage connected to the ESP, and the CW calculation voltage without load as seen in Figure 3. This figure shows the effect of changing the regulator voltage on the CW output voltage in various circumstances. The higher the voltage regulator, the higher the resulting CW output voltage. The CW voltage without load cannot reach the calculated voltage due to the effect of the voltage drop on the CL-01 diode, where each diode has a voltage drop of 12 volts and the influence of the capacitor. The CW voltage connected to the ESP is lower than the no-load CW voltage because the ESP is included in the load. Following (15), a voltage drop is produced in the Walton Cockroft circuit due to the current flowing.

Table 2. Voltage measurement using HV 9012 probe

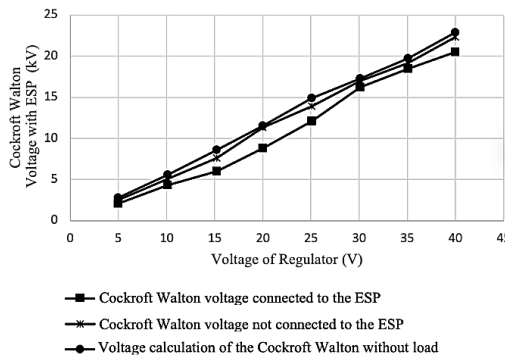| Voltage of regulator	Voltage of transformer (V)	Cockroft walton voltage without load (kV)	Cockroft walton voltage with ESP (kV)	Calculation of cockroft walton voltage (kV)
5	142	-2.5	-2.1	-2.81
10.1	283	-5.1	-4.3	-5.60
15.2	434	-7.6	-6	-8.59
20	583	-11.3	-8.8	-11.54
25.1	752	-13.9	-12.1	-14.88
30.1	874	-17	-16.2	-17.30
35.1	998	-19.2	-18.5	-19.75
40	1156	-22.3	-20.5	-22.88

Figure 3. The change from the voltage regulator to the CW voltage

3.2. Sensor testing

The sensor used to determine the efficiency of ESP capture is the particulate matter sensor (PMS) 5003. This sensor is used only to monitor levels of particulate matter whose size is smaller than 2.5 µm (PM2.5). PMS5003 will suck in the air in the exhaust stream and read how much PM2.5 is in units of ppm. The infrared diode contained in the PMS5003 will emit infrared light into the air that has been sucked. Particles exposed to infrared light will result in scattering of light. If the transmitter diode contained in PMS5003 is exposed to infrared light, a change in voltage will occur. The more transmitter diodes receive infrared light, the higher the ppm level. PMS5003 requires a microcontroller that can process the output produced by PMS5003 so that PM2.5 levels can be displayed on a laptop screen or liquid cyrstal display (LCD) monitor.

Figure 4 shown the number of PMS5003 used is two pieces located in the inlet hole and outlet hole. PMS5003 is placed specifically on a frame where the frame is attached to a pipe. The purpose of making a frame is so that it does not affect the exhaust gas flow and can only read the PM2.5 levels contained in the exhaust gas stream. Every time PMS5003 will read PM2.5 levels. PMS5003 is found in the inlet hole compared to the outlet hole. This comparison will produce the efficiency value of the ESP. According to government regulations, the permitted level of particulate matter in exhaust gases is 120 ppm. So that every PMS5003 in the outlet hole reads PM levels greater than 120, the vibrator will vibrate so that the ashes that settle on the ESP will fall out and fall. Figure 5 is a reading of particulate matter levels on a computer. In this figure, the efficiency value of the particulate matter in the exhaust gas is still below 120, so all vibrator conditions are not working (Vibrator0). Likewise, in Figure 6, with the reading of particulate matter levels on the LCD monitor, the vibrator is turned off.
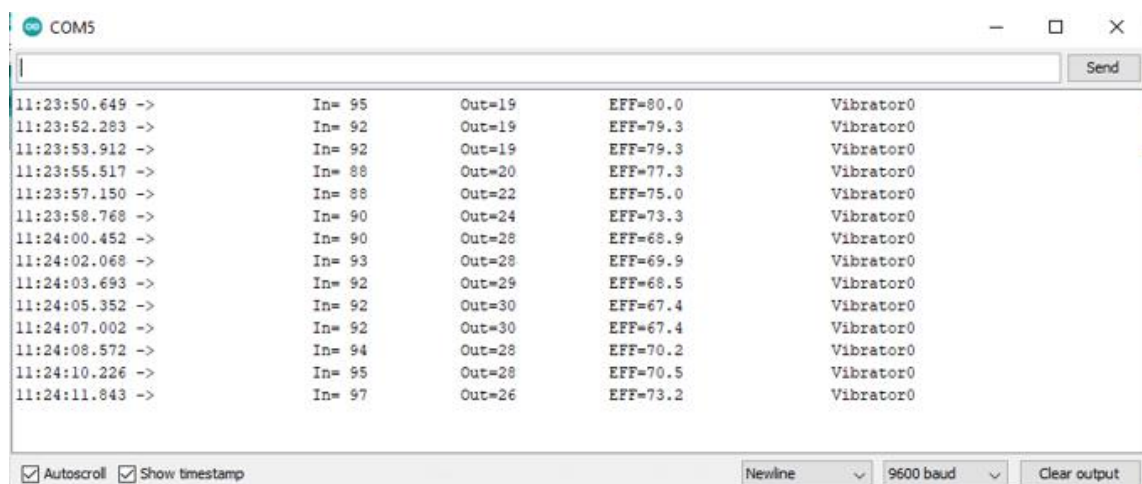

Figure 4. Frame PMS5003

Figure 5. Particulate matter levels on the compuer

Figure 6. Particulate matter levels on the LCD monitor

3.3. Effect of voltage on efficiency

In the ESP test, the smoke produced from burning egg nests is used as a sample. The way ESP performance works is that the ESP is supplied with high voltage. After that, the egg tray is burned in the smoke-producing room. Smoke is sucked in by the fan and sent to the ESP. Furthermore, PMS5003 in the inlet and outlet holes monitor the levels of particulate matter for 10 minutes.

3.3.1. Efficiency with a pair of electrodes

The effect of voltage on particle capture efficiency is shown in Figure 7. As seen in this figure, in the 3rd minute, the efficiency of capturing particles at each voltage appears stable. Compare the capture efficiency with the voltage by averaging the capture efficiency from 3-10 minutes. Furthermore, the graph in Figure 8 shows that the average efficiency is different for each parameter of the voltage regulator. From this figure, the highest average value for the efficiency of capturing particulate matter is found at the 35-volt regulator voltage with an average efficiency of 98.7% and an applied voltage of -18.5 kV. The lowest capture efficiency is at a voltage of 20 V with an efficiency of 98.7% with an applied voltage of -8.8 kV.
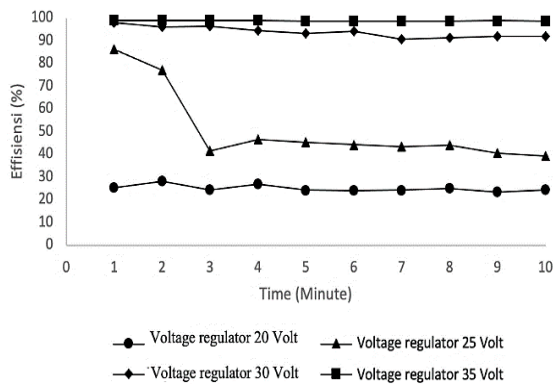
Figure 7. ESP efficiency with a pair of electrodes
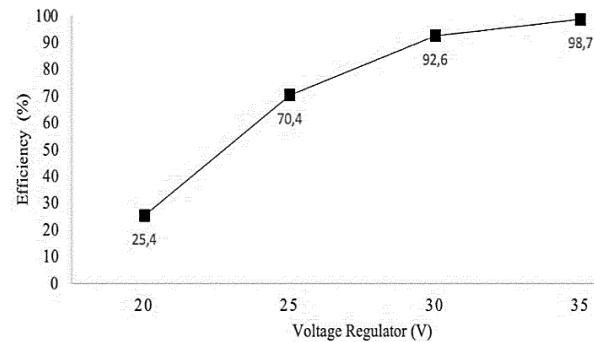
Figure 8. ESP average efficiency of a pair of electrodes

3.3.2. Efficiency with two pairs of electrodes

Figure 9 describes the configuration has a large influence on particle efficiency. As seen in this figure, in the 2nd minute, the efficiency of capturing particles at different voltages is stable. By averaging the capture efficiency from 2-10 minutes, it can be compared to the capture efficiency with the amount of voltage, as illustrated in Figure 10. Furthermore, the graph in Figure 10. shows that the average efficiency is different for each parameter of the voltage regulator. From the graph, the highest average efficiency for capturing particulate matter is found at a 30-volt regulator voltage with an average efficiency of 99.5% at an applied voltage of -16.2 kV. The lowest capture efficiency is at a voltage of 20 V with an efficiency of 90.6% applied voltage of 8.8 kV.
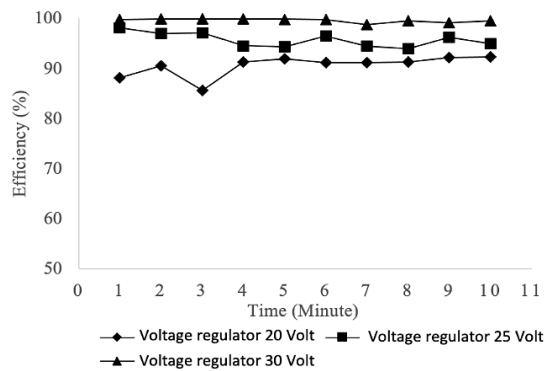
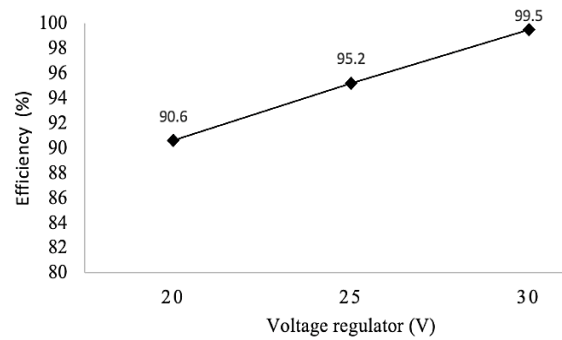Figure 9. ESP efficiency with two pairs of electrodes

Figure 10. ESP average efficiency of two pairs of electrodes

3.4. Efficiency with two pairs of electrodes

There are differences in efficiency values between the two configurations that have been done. These differences can be observed in the graph in Figure 11. As seen in this figure, the highest efficiency voltage in each sample is always on the ESP with two pairs of electrodes. It will be feasible to use on ESP with a pair of electrodes if the regulator ladder is 35 volts. Meanwhile, ESP with two pairs of electrodes is suitable for use when the voltage regulator is 30 volts. Whether or not ESP is appropriate depends on the PM levels in the exhaust gas. If the PM level exceeds 120 ppm, then ESP is not feasible. The measurement results show that the two electrode configurations show that the greater the voltage, the greater the efficiency. The greater the number of pairs of electrodes, the greater the efficiency. This goes the other way around. The two configurations show a big difference in efficiency even though the voltage used is the same. Things that affect these differences are the influence of air velocity and the area of the collector. The airflow velocity will be halved on the ESP with two pairs of electrodes so that the airflow velocity is smaller than the ESP with a pair of electrodes. The lower the airflow velocity at the ESP, the higher the capture efficiency. The ESP with two pairs of electrodes has a collecting area of 2241.96 cm^3 while the ESP with a pair of electrodes has a collecting area of half that is 1120.98 cm^3. The wider the collector area, the greater the efficiency.
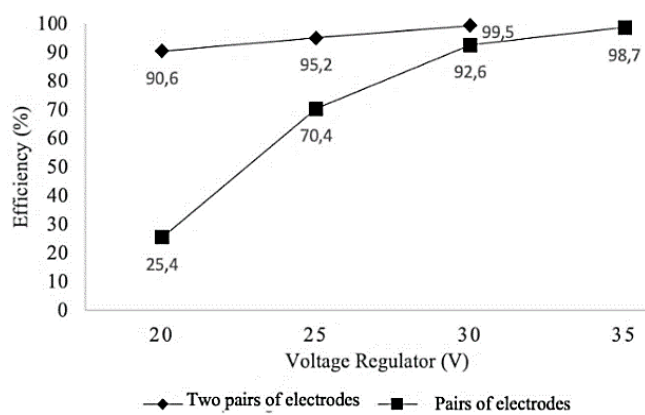

Figure 11. Comparison of the average efficiency between a pair of electrodes and two pairs of electrodes

3.5. ESP duty cycle

ESP cannot work continuously with the same efficiency. Particles that stick to the electrodes cause a decrease in efficiency. The attached particles must be cleaned from the electrodes so that the exhaust gas produced from industrial activities is not more than the allowable exhaust gas level. Based on government regulations, the permitted industrial exhaust gas content is not more than 120 ppm. This experiment used ESP with a pair of electrodes with a 40V voltage regulator. The work cycle of the ESP is observed in Figure 12.
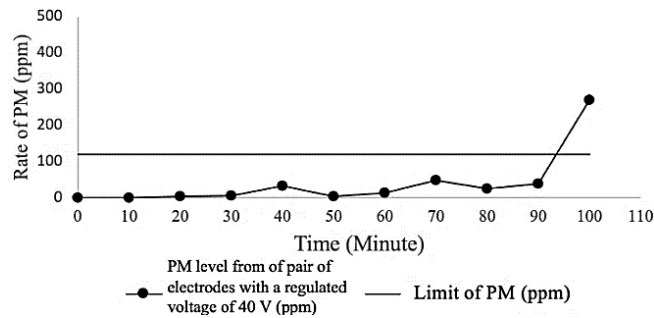
Figure 12. ESP performance with a pair of electrodes and a 40 V voltage regulator

At 70-80 minutes, the exhaust gas level has crossed the PPM limit but has decreased again. This indicates that the ESP is not working normally anymore. At 95-102 minutes, the exhaust gas level has exceeded the exhaust gas ppm limit, which is 120 ppm. This indicates that the ESP is experiencing over-capacity. Re-cleaning must be done before the ESP is used again. This indicates that the ESP with a pair of electrodes and a 40 V voltage regulator has a duty cycle of 95 minutes. After the ESP has worked for 95 minutes, it must be cleaned again.

4. CONCLUSION

As the research results, the wire-cylinder type electrostatic precipitator is close to the calculation value and can filter particulate matter in small industrial exhaust gases. Following this result, a high voltage generator with a Cockroft Walton circuit as a negative corona generator on the Electrostatic Precipitator has been made, close to the calculated value, and can be used. Furthermore, design and programming of PMS5003 can be used to monitor particulate matter levels at the inlet and outlet holes. Furthermore, by comparing PM 2.5 levels at the inlet and outlet holes, the efficiency of catching PM 2.5 on ESP is obtained. Then, the amount of voltage greatly affects the efficiency of the ESP. The greater the voltage, the greater the efficiency of the ESP. Meanwhile, ESP efficiency with two pairs of electrodes is higher than ESP with one pair of electrodes. Increasing the number of pairs of electrodes will reduce the air velocity and increase the area of the collector. Following the Regulation of the Minister of Environment and Forestry of the Republic of Indonesia number P.19/MENLHK/SETJEN/NUM.1/2/2017. ESP with a pair of electrodes will be suitable for use when the regulator voltage is greater than 35 volts, while ESP with two pairs of electrodes will be suitable for use when the regulator voltage is greater than 30 volts. The working cycle of the ESP pair of electrodes with a 40 V voltage regulator is 95 minutes. After the ESP has worked for 95 minutes, cleaning of the electrodes must be carried out. The last conclusion, installing a vibrator is unsuitable for ESPs with low-temperature exhaust gases because the resulting residue is thick and sticky, so it cannot be dropped.

REFERENCES

[1] K. Adarsh *et al.*, "Detection and real- time monitoring of sulfur dioxide concentration from automobile exhaust using IoT," in *Proceedings of the 6th International Conference on Communication and Electronics Systems, ICCES 2021*, Jul. 2021, pp. 649–656, doi: 10.1109/ICCES51350.2021.9489190.

[2] L. P. Rahayu *et al.*, "Design of gas detection toxic sulfur dioxide (SO2) in the mountain activity area," in *2019 International Conference on Advanced Mechatronics, Intelligent Manufacture and Industrial Automation, ICAMIMIA 2019 - Proceeding*, Oct. 2019, pp. 272–276, doi: 10.1109/ICAMIMIA47173.2019.9223405.

[3] P. Bürger and U. Riebel, "Electrostatic charging and precipitation of nanoparticles in technical nitrogen: Highly efficient diffusion charging by hot free electrons," *Journal of Aerosol Science*, vol. 141, p. 105495, Mar. 2020, doi: 10.1016/j.jaerosci.2019.105495.

[4] J. H. Sung, S. Kim, S. Kim, B. Han, Y. J. Kim, and H. J. Kim, "Development of an integrated electrostatic precipitator and wet scrubber system for controlling noxand particulate matter emissions from a semiconductor manufacturing process," *IEEE Transactions on Industry Applications*, vol. 56, no. 6, pp. 7012–7019, Nov. 2020, doi: 10.1109/TIA.2020.3023670.

[5] A. Y. Lusiandri, A. E. Kristiyono, and K. L. Waskito, "The application of electrostatic precipitator (ESP) as pollutant reduction in ship," *Research, Society and Development*, vol. 8, no. 12, p. e148121650, Sep. 2019, doi: 10.33448/rsd-v8i12.1650.

[6] Y. Lee, Y. S. Kim, B. Han, Y. J. Kim, and H. J. Kim, "Minimizing the size and ozone emission of electrostatic precipitators using dielectric and rolled carbon film coatings," *IEEE Transactions on Industry Applications*, vol. 58, no. 1, pp. 753–759, Jan. 2022, doi: 10.1109/TIA.2021.3122402.

[7] Y. Lee, J. H. Sung, B. Han, Y. J. Kim, and H. J. Kim, "Particle removal performance of a two stage electrostatic precipitator with carbon based nonmetallic collection plates for oil mist," in *2020 IEEE Industry Applications Society Annual Meeting, IAS 2020*, Oct. 2020, pp. 1–7, doi: 10.1109/IAS44978.2020.9334890.

[8] H. Lee *et al.*, "Development of electrostatic-precipitator-type air conditioner for reduction of fine particulate matter in subway," *IEEE Transactions on Industry Applications*, vol. 58, no. 3, pp. 3992–3998, May 2022, doi: 10.1109/TIA.2022.3160125.

[9]   J. He, G. Xu, X. Zhou, and L. Xu, "Application of five stages electrostatic precipitation technology in renovation of dust-collector for power station boiler," in *2010 4th International Conference on Bioinformatics and Biomedical Engineering, iCBBE 2010*, Jun. 2010, pp. 1–4, doi: 10.1109/ICBBE.2010.5515988.

[10]   M. Badran and A. M. Mansour, "Evaluating performance indices of electrostatic precipitators," *Energies*, vol. 15, no. 18, p. 6647, Sep. 2022, doi: 10.3390/en15186647.

[11]   D. Anggoro, M. Saefuddin, I. Fatimah, S. Indrawati, Sudarsono, and Nurrisma, "Optimization of high temperature furnace system as one of the spray pyrolisis subsystems based on R type thermocouples and PID control," *Journal of Physics: Conference Series*, vol. 1153, no. 1, p. 012037, Feb. 2019, doi: 10.1088/1742-6596/1153/1/012037.

[12]   A. Bologa, A. Hornung, H. Seifert, K. Woletz, and H. R. Paur, "Application of space-charge electrostatic precipitator for collection of oil mist from pyrolysis gases," in *2008 IEEE International Conference on Dielectric Liquids, ICDL 2008*, Jun. 2008, pp. 1–4, doi: 10.1109/ICDL.2008.4622490.

[13]   A. Afshari *et al.*, "Electrostatic precipitators as an indoor air cleaner a literature review," *Sustainability (Switzerland)*, vol. 12, no. 21, pp. 1–20, Oct. 2020, doi: 10.3390/su12218774.

[14]   M. Okubo, T. Yamamoto, T. Kuroki, and H. Fukumoto, "Electric air cleaner composed of nonthermal plasma reactor and electrostatic precipitator," *IEEE Transactions on Industry Applications*, vol. 37, no. 5, pp. 1505–1511, 2001, doi: 10.1109/28.952528.

[15]   Y. Lee, Y. S. Kim, B. Han, Y. J. Kim, and H. J. Kim, "Extremely low ozone emission electrostatic compact air purifier using carbon fiber ionizers and carbon film collection stage," in *2020 IEEE Industry Applications Society Annual Meeting, IAS 2020*, Oct. 2020, pp. 1–7, doi: 10.1109/IAS44978.2020.9334757.

[16]   P. Wang, C. Li, J. Li, M. Zhang, Y. Yang, and K. Yu, "Electrostatic effects of corona discharge on the spectrum and density evolution of water droplets in air," *IEEE Access*, vol. 8, pp. 196264–196273, 2020, doi: 10.1109/ACCESS.2020.3034264.

[17]   Y. Shi *et al.*, "Numerical study of the effect of temperature and H2O concentration on the electrostatic precipitator characteristics at high temperatures," *Powder Technology*, vol. 411, p. 117913, Oct. 2022, doi: 10.1016/j.powtec.2022.117913.

[18]   N. Rani, J. Kaur, H. Bhatia, S. S. Saini, R. Kaur, and E. Sidhu, "Design and performance analysis of cockroft-walton voltage multiplier (CWVM) energy harvesting for low power applications," in *Progress in Electromagnetics Research Symposium*, May 2017, pp. 2131–2136, doi: 10.1109/PIERS.2017.8262103.

[19]   R. Muljana, L. D. Ayuningtyas, R. P. Daksa, S. F. Djamhari, M. A. Fiezayyan, and N. T. M. Sagala, "Air pollution prediction using random forest classifier: a case study of DKI Jakarta," in *ICCoSITE 2023 - International Conference on Computer Science, Information Technology and Engineering: Digital Transformation Strategy in Facing the VUCA and TUNA Era*, Feb. 2023, pp. 428–433, doi: 10.1109/ICCoSITE57641.2023.10127759.

[20]   K. Wattal and S. K. Singh, "Multivariate air pollution levels forecasting," in *ACCESS 2021 - Proceedings of 2021 2nd International Conference on Advances in Computing, Communication, Embedded and Secure Systems*, Sep. 2021, pp. 165–169, doi: 10.1109/ACCESS51619.2021.9563281.

[21]   S. F. Salleh, A. Khan, C. N. Hipolito, L. Kinidi, and D. S. H. A. Hardin, "An analytical modeling approach for performance evaluation of electrostatic precipitator (ESP)," *Journal of Energy and Safety Technology (JEST)*, vol. 1, no. 2–2, Feb. 2019, doi: 10.11113/jest.v1n2-2.33.

[22]   A. Pal, A. Dixit, and A. K. Srivastava, "Design and optimization of the shape of electrostatic precipitator system," *Materials Today: Proceedings*, vol. 47, pp. 3871–3876, 2021, doi: 10.1016/j.matpr.2021.03.448.

[23]   E. T. Nghishiyeleke, V. M. Kemba, A. M. S. Endunde, and M. M. Mashingaidze, "Design of an electrostatic precipitator for a novel bituminous coal-fired circulating fluidised bed combustion power plant in Namibia," *Journal of Energy in Southern Africa*, vol. 31, no. 3, pp. 38–57, Oct. 2020, doi: 10.17159/2413-3051/2020/v31i3a8752.

[24]   X. Wei, Z. Shen, Y. Ye, J. Leng, Z. Xu, and L. Jin, "Optimization and design of a high-voltage supply for electrostatic precipitators," in *ECCE 2020 - IEEE Energy Conversion Congress and Exposition*, Oct. 2020, pp. 2268–2275, doi: 10.1109/ECCE44975.2020.9235595.

[25]   Z. He and E. T. M. Dass, "Correlation of design parameters with performance for electrostatic Precipitator. Part I. 3D model development and validation," *Applied Mathematical Modelling*, vol. 57, pp. 633–655, May 2018, doi: 10.1016/j.apm.2017.05.042.

[26]   V. Thonglek and T. Kiatsiriroat, "Use of pulse-energized electrostatic precipitator to remove submicron particulate matter in exhaust gas," *Journal of Engineering and Technological Sciences*, vol. 46, no. 3, pp. 271–285, Sep. 2014, doi: 10.5614/j.eng.technol.sci.2014.46.3.3.

[27]   W. E. Abdel-Azim, A. A. Elserougi, and A. A. Hossam-Eldin, "A modular switched-capacitor voltage multiplier-based multi-module high-voltage pulse generator for electrostatic precipitators applications," *Alexandria Engineering Journal*, vol. 65, pp. 503–520, Feb. 2023, doi: 10.1016/j.aej.2022.09.028.

BIOGRAPHIES OF AUTHORS

Yulianta Siregar [ID] [SC] was born July 09, 1978 in Medan, North Sumatera Utara, Indonesia. He did his undergraduate work at University of Sumatera Utara in Medan, North Sumatera Utara, Indonesia. He received a Bachelor of Engineering in 2004. After a while, he worked for a private company. He continued taking a master's program in Electrical Engineering at the Institute of Sepuluh Nopember, Surabaya, West Java, Indonesia, from 2007-2009. He was in a Ph.D. program at Kanazawa University, Japan, from 2016-2019. Until now, he lectured at Universitas Sumatera Utara. He can be contacted at email: julianta_srg@usu.ac.id.

Bio Debataraja is a fresh graduate of Electrical Engineering bachelor's degree from Universitas Sumatera Utara in 2022. His research area field study is a high voltage, and electrical power system. He can be contacted at email: biodebataraja@gmail.com.

Soeharwinto his Ph.D. Student in Electrical Engineering, Universitas Sumatera Utara, Indonesia (Now). Master in computer networks, Institut Teknologi Bandung, (2001). Bachelor degree in Electrical Engineering, University of Sumatera Utara, Indonesia (1996). Lecturer in University of Sumatera Utara, Indonesia, since 2000. He can be contacted at email: soeharwinto@usu.ac.id.

Naemah Mubarakah received the B.Sc. degrees in electrical power engineering from University of Sumatera Utara, Medan, Indonesia (1998~2004), master's program in Electrical Engineering at the Institute of Sepuluh Nopember, Surabaya, West Java, Indonesia, from (2007-2009). She continued taking a Ph.D. Student at Universitas Sumatera Utara, Indonesia (2018-Now). She can be contacted at email: naemah.mubarakah@gmail.com.

Riswan Dinzi received the B.Sc. degrees in electrical power engineering from University of Sumatera Utara, Medan, Indonesia (1979~1985), master's program in Electrical Engineering at the Institut Teknologi Bandung, Indonesia, from (1994–1996). He is associatedd professor at Universitas Sumatera Utara, Indonesia, since 1988. He can be contacted at email: dinziriswan@gmail.com.